Research papers

Does the creation of a boreal hydroelectric reservoir result in a net change in evaporation?

Ian B. Strachan [a,*], Alain Tremblay [b], Luc Pelletier [a], Simon Tardif [b], Christian Turpin [b], Kelly A. Nugent [a]

[a] Department of Natural Resource Sciences, McGill University, Sainte-Anne-de-Bellevue, Québec, Canada
[b] Hydro-Québec, Montréal, Québec, Canada

ARTICLE INFO

ABSTRACT

Estimates of water consumption from hydroelectricity production are hampered by a lack of common methodological approaches. Studies typically use gross evaporation estimates which do not take into account the evaporative water loss from the pre-flooded ecosystems that would occur without the presence of a reservoir. We evaluate the net change in evaporation following the creation of a hydroelectric reservoir located in the Canadian boreal region. We use a direct measurement technique (eddy covariance) over four different ecosystems to evaluate the pre- and post-flood landscape water flux over a five-year period. The net effect of reservoir creation was to increase evaporation over that of the pre-flooded ecosystem. This change was dependent both on management and differences in the timing of the evaporation with nighttime and autumn contributing strongly to the reservoir evaporation. Managed reduction of water level, and thus the evaporating area, reduced the evaporation.

1. Introduction

Evaporation (E) and evapotranspiration (ET) represent important elements of the water balance in terrestrial and aquatic boreal ecosystems (Baldocchi et al., 1997; Blanken et al., 2000; Humphreys et al., 2006). The controls on, and rates of, E and ET vary between the different ecosystems that characterise the boreal landscape (e.g. forests, peatlands and aquatic features) largely due to the difference in biophysical characteristics in these environments. In water bodies, the controls on E are physical, being functions of temperature, wind speed, vapour pressure and radiation (Penman, 1948; McVicar et al., 2012; McMahon et al., 2013). Vegetative systems with vascular plants exert control on water loss through stomata. In forests, the water loss to the atmosphere is a combination of E from soil and wet vegetative surfaces, and transpiration from the canopy and understorey. While the E component is strongly linked to precipitation (P), the soil water holding capacity, as well as stand type, age and structure affecting the precipitation interception (Jassal et al., 2009) also play an important role. Transpiration in taller mature forests is mainly controlled by vapour pressure deficit (VPD) (e.g. McLaren et al., 2008), as

these aerodynamically rougher surfaces are more coupled to changes in the atmosphere (Jarvis and McNaughton, 1986) and induce stomatal control on trace gas exchange. In peatlands, available energy has been identified as the primarily control on ET, with VPD having some control on sites with greater abundance of vascular plants (Kurbatova et al., 2002; Humphreys et al., 2006). Although the water table in peatlands is typically close to the surface, the ET rates are lower than E rates calculated for open water (Lafleur and Roulet, 1992). Water supply to the surface has been shown to restrict ET rates when the water table moves farther from the surface (Lafleur et al., 2005).

Land-use change, such as the construction of a large water reservoir in boreal regions for hydroelectricity production, can affect E and ET by changing the pre-existing land surface cover from a combination of terrestrial (forest and wetlands) and aquatic (lakes and rivers) ecosystems to a single large water body. Recently, the hydro industry has begun to evaluate the additional evaporative loss created by the land-cover change to reservoir in the energy production cycle in order to further evaluate the net costs of hydroelectricity production. In a review of published estimates of this evaporative water loss (termed 'consumption') from hydroelectricity production, Bakken et al. (2013) compiled results of gross annual rates of E from reservoirs. Several other studies report partial year estimates of reservoir E (e.g. Tanny et al.,

2011). Bakken et al. (2013) also noted large variation in estimates per unit energy produced ($\sim$0 to 209 m^3 MW h^{-1}), highlighting a lack of common methodological approaches. More importantly, studies (e.g. Mekonnen and Hoekstra, 2012; Torcellini et al., 2003; Yesuf, 2012) typically use gross E estimates which do not take into account the evaporative water loss from the pre-flooded ecosystems that would occur without the presence of the reservoir. In fact, globally, there are few studies reporting eddy covariance (EC) measurements of E from water bodies (Table 1) with most restricted to the open water season; we could find only two previous studies (Spence et al., 2013; Spence and Hedstrom, 2015) reporting continuous measurements over several complete years. The E rates generally follow the expected trend of higher amounts in the tropics and decreasing in colder climatic zones. A host of E studies (including several long term; e.g. Lenters et al., 2005) are available which do not report EC measurements of the evaporative flux itself (e.g. energy budget based on meteorological variables). Still other studies focus on carbon (e.g. Buffam et al., 2011) rather than E.

In the present study, we evaluate the net change in water vapour transfer to the atmosphere following the creation of a hydroelectric reservoir located in the Canadian boreal region. We use a direct measurement technique (eddy covariance), which provides semi-continuous ecosystem scale measurements of latent heat flux density (Q_E), over four different ecosystems to evaluate the pre- and post-flood landscape flux over a five-year period. Our objectives were: (1) document the variability in Q_E for the dominant natural ecosystems in the boreal region where hydro-electricity is produced; (2) provide an estimate of the annual evaporation from the reservoir; and, (3) evaluate the net impact of reservoir creation on water flux to the atmosphere.

2. Material and methods

2.1. Study region and description

The study region is located in the James Bay lowland, in boreal Québec, Canada, at the northern limit of the closed boreal forest. While no long-term direct measurements of temperature and precipitation data are available for the region, the interpolated mean temperature and precipitation ($\pm$ standard error) of the National Land and Water Information Service for the period 1971–2000 (NLWIS, Hutchinson et al., 2009) are $-2.3 \pm 0.2\,°C$ and 735 ± 12 mm. The coldest and warmest months are January ($-22.1 \pm 0.5\,°C$) and July ($14.6 \pm 0.2\,°C$), respectively. The natural landscape prior to the impoundment of the Eastmain-1 reservoir was composed of both aquatic and terrestrial ecosystems (Teodoru et al., 2012). The aquatic ecosystems (Eastmain river, lakes and streams) represented 25% of the pre-flooded area with the Eastmain river representing about 55% of the surface covered by aquatic ecosystems, lakes 45% and streams less than 1%. Forests and wetlands dominated the natural terrestrial ecosystems. Forests were 49% of the pre-flooded landscape; with 56% of forest being coniferous, 5% deciduous and 38% having been burned. Wetlands covered 18% of the pre-flooded reservoir area with bog peatlands dominating at 77%. The remaining wetland surface was composed of swamps or marshes (22%) and fen peatlands (less than 1%). The remaining 8% of the pre-flooded reservoir area was classified as non-forest, representing outcrops, blockfields or other non-vegetated quaternary deposit surfaces.

2.2. Sites, instrumentation and flux calculations

We used the eddy covariance (EC) technique (Baldocchi, 2003) to measure Q_E at four sites (Table 2; Fig. 1; system components

described below). Note that we will refer to water vapour transfer as E and use depth/time units for daily or annual sums and volume units in the context of energy production. Three sites are analogues representing pre-flooded mature forest (FOR), pre-flooded burned forest (BUR), and pre-flooded peatland (BOG). FOR is dominated by black spruce (*Picea mariana*) with a mean age of 84 years (as of 2011). The forest floor and understory were dominated by *Lichen* spp., *Pleurozium schreberi* and shrubs (*Rhododendron groenlandicum, Vaccinium myrtilloides, Kalmia polifolia* and *Kalmia angustifolia*). BUR is a post-fire re-growth dominated by jack pine (*Pinus banksiana*) seedlings with an average height of 0.35 m (as of 2011). The pre-fire forest was dominated by jack pine, common on the drier portions of the regional landscape, whereas *P. mariana* dominates the wetter locations. The 2005 fire resulted in complete death of the canopy and understory with charred tree stems remaining standing. The ecosystem now features active re-growth of jack pine saplings with other species including Labrador Tea (*R. groenlandicum*), Sheep Laurel (*K. angustifolia*), Canadian blueberry (*V. myrtilloides*) and clubmoss (*Lycopodium digitatum*). BOG is an ombrotrophic bog that covers approximately 2.2 km^2. The site is dominated by *Sphagnum* species (e.g. *Sphagnum fuscum, Sphagnum cuspidatum, Sphagnum fallax*) and Ericaceous shrubs (e.g. *Chamaedaphne calyculata, K. angustifolia, R. groenlandicum* and *Andromeda glaucophylla*). More details on BOG can be found in Pelletier et al. (2011), van Bellen et al. (2011) and Strachan et al. (2016).

The EM-1 hydroelectric reservoir was created in 2005 by flooding a section of boreal terrestrial landscape. It is a shallow reservoir with a mean depth of 6 m and a water residence time of approximately 3.5 months. The Eastmain-1 powerhouse was commissioned in 2006 and has a total capacity of 1248 MW (as of 2011). The main dam and 33 dikes form the Eastmain-1 Reservoir, with a maximum water surface area of 627 km^2. The post-flooding fluxes were determined from an EC system (RES) mounted on a scaffold tower located on an island in the middle of the reservoir.

We report measurements of Q_E and sensible heat flux density (Q_H) taken from January 2008 to October 2012 at RES and FOR, from June 2008 to October 2012 at BOG, and from June to September, 2011 and March to September, 2012 at BUR. The EC system at each of the four sites consisted of a three-dimensional sonic anemometer-thermometer (CSAT-3, Campbell Scientific, Logan, UT), an open-path infrared gas analyzer (IRGA; Li-7500, LI-COR, Lincoln, NE) and a fine wire thermocouple (FW03, Campbell Scientific, Logan, UT). The variables used to calculate the flux were measured at 10 Hz and fluxes were calculated for 30-min periods. The sampling frequency was reduced to 5 Hz from November to April to avoid overwriting data cards/missing data caused by limited access for retrieving data during the winter. All sites were accessed by helicopter except BUR which was located near a gravel access road. EC data were stored on compact flash cards using a data logger (CR5000, Campbell Scientific, Logan, UT) and the data were downloaded on average every one to two months.

In computing turbulent fluxes, a two-axis coordinate rotation was applied (Baldocchi et al., 1997), de-spiking was performed using the high frequency data (Vickers and Mahrt, 1997), and detrending was done using the block average method (Baldocchi, 2003). Finally, the effect of fluctuations in air density was removed (Webb et al., 1980). The fluxes are presented following the micrometeorological convention where a loss of H$_2$O to the atmosphere is represented by a positive flux, while a gain to the ecosystem is represented by a negative flux. At terrestrial sites, supporting measurements of meteorological variables included incoming and outgoing solar and longwave radiation (CNR-1; Kipp and Zonen, Delft, Netherlands), incoming and reflected photosynthetically active radiation (PAR; LI-190SB; LI-COR, Lincoln, NE), rainfall (TE525M tipping bucket rain gage; Texas

Table 1

Summary of published studies using eddy covariance tower flux estimates of evaporation over water surfaces. Studies are reported chronologically and then alphabetically. Abbreviations: E = evaporation; EB = energy balance; EC = eddy covariance; nr = not reported.

Study	Type	Location/climate	Objectives	E rate (time period)	Main findings (related to E)
1. Smith (1974)	Lake	Ontario, Canada/Hot summer continental	Calculate momentum, heat, E from the surface of Lake Ontario	nr	(1) Fluxes substantially the same as reported in literature to date for similar wind speeds and stability
2. Friehe and Schmitt (1976)	Ocean	Various ocean locations	Combine four data sets and compare E from EC with profile data	nr	(1) Adequate agreement found (2) Lack of high wind speed measurements limits applicability
3. Anderson and Smith (1981)	Ocean	Sable Island, Nova Scotia/Oceanic	Measure E over ocean surface extending range of available conditions	−0.008 to 0.051 g m^{-2} s^{-1} (4 days over 3 years)	(1) Rate of E can be represented by a bulk formula (2) Need for reliable EC measurements at higher wind speed in open ocean
4. Katsaros et al. (1987)	Ocean	Dutch coast/ Oceanic	Measure E over open ocean at moderate to high wind speeds	nr	(1) E became small during highest wind conditions when atmospheric humidity was high (2) Moisture carried principally by spray to heights above sensors
5. Ikebuchi et al. (1988)	Lake	Japan/Humid subtropical	Compare methods to estimate E	540 mm yr^{-1}	(1) Bulk transfer method is the most reliable (2) E is large from September to March and small the rest of the year (3) Adjusting E by wind speed can yield E over the whole lake surface
6. Smith (1989)	Ocean	Various locations	Review measurements of E over open ocean to date	nr	(1) E from EC, profile and spectral dissipation methods agree (2) No reliable high wind speed measurements of E available
7. Sene et al. (1991)	Lake	Indonesia/tropical	Measure E and develop methods to estimate past E using historical meteorological data	1500 mm yr^{-1}	(1) Instantaneous rate of E linked to the wind speed (2) EB methods could be used to estimate E
8. Stannard and Rosenberry (1991)	Lake	Nebraska, USA/ semi-arid	Compare EC with EB on 30-min basis	nr	(1) Agreement between EC and EB methods using weighted energy storage, accounting for tower source area
9. Assouline and Mahrer (1993)	Lake	Israel/ Mediterranean	Compare EC with EB on 30-min basis	4.1 mm d^{-1} (May–June) 5.7 mm d^{-1} (September– October)	(1) Wind speed and stability strongly affect E (2) Large differences between measured and estimated E in terms of timing and rates
10. DeCosmo et al. (1996)	Ocean	Dutch coast/ Oceanic	Measure E over open ocean	nr	(1) Measurements of E up to wind speeds of 18 ms^{-1} were successfully made
11. Venäläinen et al. (1998)	Lake	Sweden/warm summer continental	Evaluate the importance of sheltering due to forests on E from small lakes	nr	(1) LE increases with increase of over-water fetch due to the increase of wind speed in lakes <10 km^2 (2) Sheltering is small in large lakes with fetches of several km's
12. Heikinheimo et al. (1999)	Lake	Sweden/ warm summer continental	Improve parameterisation of the lake-atmosphere interaction	Lake Tämnaren: 281 mm Lake Råksjö: 271 mm (May–October)	(1) High E rates even during stable stratification (2) Variation in LE flux correlated with wind speed (3) Higher E measured on the large lake compared to the sheltered smaller lake under strong wind conditions
13. Blanken et al. (2000)	Lake	Northwest Territories, Canada/continental subarctic	Measure E from large high-latitude lake	386 and 485 mm (ice free period only)	(1) Episodic E events linked to high winds and cold fronts (2) Positive LE flux during ice free period once surface temperature reaches 4 °C
14. Blanken et al. (2003)	Lake	Northwest Territories, Canada/continental subarctic	Study the effect of entrainment of warm, dry air on E	nr	(1) Short-term episodic E events are significant contributors to the seasonal E total (2) Maximum E is just before the lake freezes when lake to air vapour pressure gradient is maximum
15. Eichlinger et al. (2003)	Reservoir	New Mexico, USA/ Cold desert	Develop a methodology for estimating E from open water	3 mm d^{-1} (~1 year)	(1) Proposed method and EC differed by 8% during an intensive measurement period
16. Rouse et al. (2003)	Lake	Northwest Territories, Canada/continental subarctic	Expand previous work with a longer term study	384–506 mm (ice-free periods of three years)	(1) Surface radiation budget and convective fluxes are not related on day-to-day basis (2) From ice-melt to late summer, stable atmosphere is linked to small E; through fall, unstable atmosphere causes larger E (3) The date of ice-melt is the largest single control on seasonal thermal and energy regimes

Table 1 (continued)

Study	Type	Location/climate	Objectives	E rate (time period)	Main findings (related to E)
17. Beyrich et al. (2006)	Lake	Germany/Maritime temperate	Measure H and LE over different surface types using EC; compare aggregated surface fluxes with area-averaged flux estimates from scintillometer and Helipod measurements	nr (May–June)	(1) Substantial flux differences between the major land-use classes in the area (2) Variability of the surface fluxes between the different types of land use was larger for H than for LE (3) H and LE can be aggregated from land-use weighted local EC measurements over relevant surface types
18. Panin et al. (2006)	Lake	Germany/Maritime teperate	Parameterize E in small lakes considering the use of scales in weather forecast and climate models	nr (May–June)	(1) Different approaches for H and LE for the open ocean under low wind conditions with an extension for shallow water conditions show very similar results for a lake (2) The effect of the increase of fluxes for shallow lakes is on the order of 20%
19. Vesala et al. (2006)	Lake	Finland/continental subarctic	Study the magnitude and diurnal patterns in LE and compare with earlier observations	nr	(1) Strong diurnal pattern in LE except in Oct–Nov (2) LE fluxes in agreement with earlier studies
20. Assouline et al. (2008)	Reservoir	Israel/Mediterranean; Switzerland/Oceanic temperate	Explore flow statistics of H and LE over water bodies differing in climate, thermal inertia and degree of advective conditions	nr	(1) In the lake, advection is small (2) For the reservoir, the role of advection is sufficiently large to overcome the active role of temperature predicted
21. Rouse et al. (2008)	Lake	Northwest Territories, Canada/subarctic	Compare two lakes in terms of their hydrodynamic and thermodynamic behaviour	Great Slave Lake (175 days): 2.16 mm d^{-1} Great Bear Lake (139 days): 0.43 mm d^{-1} (open-water season)	(1) E from Great Slave > E from Great Bear during their respective open-water periods (2) The two lakes have dissimilar hydrological regimes linked to their different drainage basin, outflow magnitude, ice breakup timing
22. Tanaka et al. (2008)	Ocean	Southwestern Japan/Warm oceanic-humid subtropical	Study the development of the atmospheric boundary layer over sea	~2 mm d^{-1} (two weeks)	(1) E flux similar between EC and bulk transfer methods (2) Sea surface was a large energy sink during the observation period
23. Tanny et al. (2008)	Reservoir	Israel/Mediterranean	Determine E from a small reservoir and compare several approaches	5.48 mm d^{-1} (21 days not continuous; July–September)	(1) Best agreement between EC and models was using Penman (2) Water heat flux important on EB on daily basis (3) Mass transfer coefficient strongly related to wind speed (4) Pan E overestimates EC
24. Liu et al. (2009)	Reservoir	Mississippi, USA/Temperate (hot summer, no dry season)	Understand how environmental variables and meteorological conditions affect diurnal, intra-seasonal, and seasonal variations in the surface EB and E in a cool season	2.8 mm d^{-1} (September–January)	(1) Combining thermal and mechanical mixing resulted in positive LE during entire cool season (2) Nighttime evaporative water losses were substantial, contributing to 45% of the total (3) Cold fronts with windy, cold, and dry air masses resulted in larger LE
25. McGowan et al. (2010)	Ocean	Northeast Australia/Tropical monsoon	First in situ measurements of EB on the Great Barrier Reef using EC	1–3.5 mm d^{-1} (several select days)	(1) >80% of available net radiation went to heating the water and reef (2) Cold air advection during winter had the greatest impact on E
26. Mengistu and Savage (2010)	Reservoir	South Africa/Temperate (warm summer, no dry season)	Calibrate the surface renewal (SR) and renewal model methods against EC and evaluate their performance for estimating LE	1–3 mm d^{-1} (July)	(1) LE from SR and renewal model and EC were almost the same in magnitude as the available energy because of the small H during the winter measurement period
27. Blanken et al. (2011)	Lake	North Central USA/Cold continental	Describe the annual EB and discuss how the physical processes may be affected by climate change	464 and 645 mm yr^{-1}	(1) Winter E loss events 2–3 days long associated with stored heat release (2) 70 to 88% of E occurred Oct–March; (3) E best described by wind speed and vapour pressure (4) 5-month delay between maximum energy input (summer) and energy output (winter)
28. Liu et al. (2011)	Reservoir	Mississippi, USA/Temperate (hot summer, no dry season)	Evaluate the importance of cold fronts on surface EB components during two cool seasons	2007: 2.43 mm d^{-1} 2008: 2.45 mm d^{-1} (mean monthly average September–March)	(1) High-wind events promoted turbulent exchange of LE both mechanically and thermally, leading to pulses that were larger than on non-pulse days

Table 1 (continued)

Study	Type	Location/climate	Objectives	E rate (time period)	Main findings (related to E)
29. McJannet et al. (2011)	Reservoir	Queensland, Australia/Humid subtropical	Describe a methodology for using scintillometry over open water	2.5–6.5 mm d^{-1} (18 days of measurement)	(1) Excellent agreement between scintillometer and EC measurements of E
30. Nordbo et al. (2011)	Lake	Finland/continental subarctic	Determine energy closure and individual flux terms along with the driving factors	nr	(1) Diurnal variation in LE linked to VPD (2) EB closure varied from 57–112%, with averages of 82% and 72% for 2006 and 2007, respectively
31. Tanny et al. (2011)	Reservoir	Israel/ Mediterranean	Investigate E for fluctuating water level and limited fetch, and identify E model in best agreement with measurements	699 mm (104 days; not continuous May–September)	(1) Penman–Brutsaert model agreed best with EC measurements for long-term prediction (2) Penman model performed best on a daily basis
32. Liu et al. (2012)	Reservoir	Mississippi, USA/ temperate (hot summer, no dry season)	Identify processes regulating E and study diurnal, intraseasonal and seasonal variations	3.1 mm d^{-1} (annual mean)	(1) LE was out of phase with the net radiation (Rn) (2) LE exceeded Rn from Sept- Jan (3) LE affected by passage of large-scale air masses
33. Spence et al. (2013)	Lake	North Central USA/ Temperate-humid continental	Investigate physical processes controlling E over time scales from months to years	520–749 mm yr^{-1} (2008–2012)	(1) Annual E strongly dependent on synoptic events during spring and autumn (2) Air temperature is a strong determinant of E and interannual variability
34. Xiao et al. (2013)	Lake	China/Humid subtropical	Quantify dependence of transfer coefficients on wind speed and the effect of submerged macrophytes	nr	(1) Transfer coefficients taken from studies in open oceans may be subject to large uncertainties when applied to inland lakes, especially in the presence of submerged macrophytes or if the lake is shallow and wind speed is low
35. McGloin et al. (2014)	Reservoir	Queensland, Australia/Humid subtropical	Compare E from EC and scintillometry	nr	(1) Scintillometer measurements of E were greater than EC; several possible explanations were postulated to account for the difference
36. Shao et al. (2015)	Lake	Ohio, USA/Warm summer continental	Understand energy exchange between the lake surface and the atmosphere	721 mm yr^{-1} (October 2011– September 2012) 646 mm yr^{-1} (October 2012– September 2013)	(1) 35% of the variation in half hourly LE explained by VPD (2) E returns approximately 90% of annual rainfall to the atmosphere
37. Spence and Hedstrom (2015)	Lake	British Columbia, Canada/Humid continental	Address uncertainly in E rates through describing controlling variables, seasonal cycles and annual rates	725–835 mm yr^{-1} (2011–2014)	(1) Annual E cycle follows variation in water temperature, surface to air vapour pressure difference and atmospheric stability (2) E rates are highest in August and lowest in April
38. This study	Reservoir	Québec, Canada/continental subarctic	Determine the change in evaporation resulting from reservoir creation	595 mm yr^{-1} (2008–12)	(1) E from reservoir is larger than E from the weighted surfaces that were flooded (2) Net result of land-use change is smaller than the gross reservoir E because pre-flooded surfaces were source of E to atmosphere

Electronics, Dallas, TX), wind speed and direction (wind monitor 05103; RM Young, Traverse City, MI), air temperature and relative humidity (HC-S3; Campbell Scientific, Logan, UT), and soil temperature at 5 cm, 10 cm, 20 cm, and 40 cm (type T thermocouples). At RES, it was not possible to measure radiative fluxes over the water and therefore only downwelling fluxes were measured. All environmental variables were measured at 0.5 Hz and 30-min averages computed and stored. Each site was powered using a combination of solar panels and small wind turbines which trickle-charged a bank of deep-cycle 12-V batteries.

2.3. Data processing, quality control and gap filling procedures

We used an in-house Matlab (Mathworks, Natick, MA) script to do a first automated quality control of the 30-min flux and climate data following the established FCRN (Fluxnet-Canada Research Network) guidelines (Lafleur et al., 2005; Humphreys et al., 2006). Out-of-range data points and those falling into a period of known instrument malfunctioning or servicing were eliminated. The built-in IRGA diagnostic signal was used to identify unreliable data due to obstruction of the IRGA's path caused primarily by precipitation events. The quality control procedure followed Bergeron and Strachan (2011). At the terrestrial sites, nighttime (defined as incoming shortwave radiation <10 W m^{-2}) flux data were rejected when friction velocity (u^*) was below site-specific threshold values (Table 2), determined based on the technique described in Mkhabela et al. (2009). No u^* threshold was applied to the reservoir data; under low wind speed conditions, the large thermal mass may still induce convection that is not mechanical (shear) in origin (Vesala et al., 2012). For the reservoir tower, data were restricted to the range of azimuthal directions (>220° and <40°) where the flux originated from water and did not include the island within the source area. Data quality controls, power loss, u^* (terrestrial) and direction (reservoir) filtering cumulatively resulted in an average of 45% of 30-min data being retained over all sites and all seasons annually. This is the same as Jonsson et al. (2008) who reported 46% retention over a Swedish lake. Our data retention during summer/ice-free daytime periods was higher and averaged 68% for all sites and years. Our values lie within the global range of 40–80% retention reported in EC studies (e.g. Papale et al., 2006; Falge et al., 2001).

Half-hourly turbulent fluxes at FOR, BUR, and BOG were gap-filled using a procedure adapted from Amiro et al. (2006). All gaps less than four half hourly periods were filled using linear interpolation. For the growing season, larger gaps were filled based on a
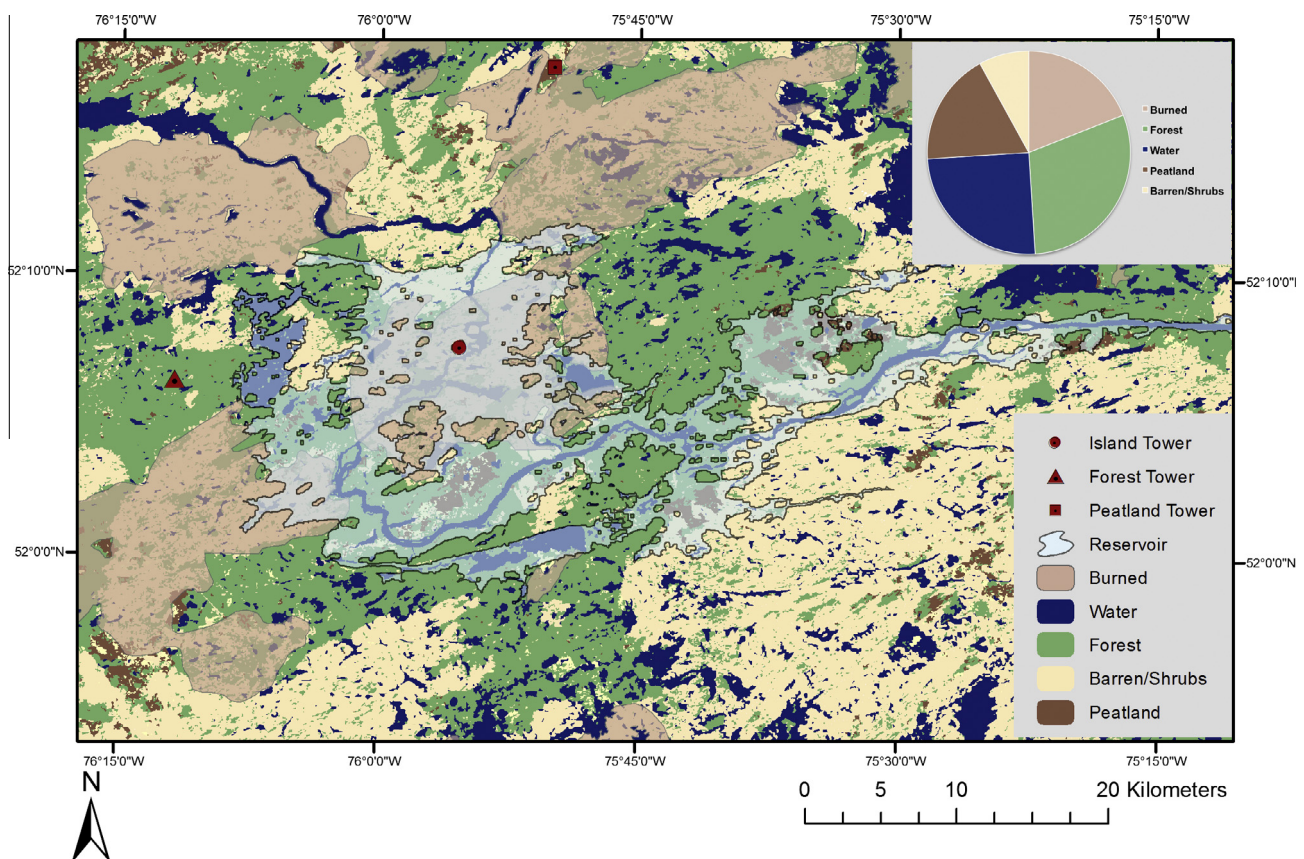
Table 2
Site descriptions, coordinates and selected properties of the flux tower locations. z_{ref} is the height of the eddy covariance instrumentation; h is the mean height of the primary live canopy; u^*_{crit} is the low-turbulence threshold for rejection of flux data.

Site	Description	Coordinates	z_{ref} (m)	h (m)	u^*_{crit}
BOG	Ombrotrophic bog	52°17′25″N 75°50′25″W	2.75	0.25	0.08
FOR	84 yr black spruce forest	52°06′16″N 76°11′48″W	23.0	10.0	0.25
BUR	Burned 7 yr Jack pine forest	52°16′12″N 76°44′53″W	6.0	0.35	0.17
RES	Reservoir island	52°07′30″N 75°55′51″W	15.0	n/a	n/a

Fig. 1. Location of the Eastmain Reservoir and the eddy covariance towers showing pre-flooded cover classes. The EC tower at the burned forest (not shown) is located 60 km direct line distance to the northwest of the Island reservoir tower. Landsat 8 OLI imagery using land cover classes ca. 2000 from Natural Resources Canada; Canada Centre for Mapping and Earth Observation. Burn information from the Canadian Forest Service, 2011 National Fire Database.

regression between the net radiation (Q^*) and Q_E and Q^* and Q_H using a five-day moving window and missing data were filled using the regression output equations. For the non-growing season, gaps were filled using a five-day mean diurnal variation (MDV), which replaces missing half-hourly periods with an average of the mean observations for that time period (Falge et al., 2001). BUR was only gap-filled for the two measurement periods. All 30-min fluxes at RES were gap-filled using a ten-day MDV. The larger window was used because of the longer gaps present as a result of the directional restrictions. At all sites, any gaps larger than the width of the MDV (largely occurring in winter) were filled using an average of the other four years for the same time period. The gap filled, 30-min datasets were summed to generate cumulative annual values.

There is no standard method for gap filling E from tower fluxes over water. While MDV is a simple approach, other techniques such as look-up tables (LuT) or marginal distribution sampling (MDS; a moving period LuT) offer alternatives which incorporate appropriate ranges of the environmental variables which control E in this case. In a review of gap filling over terrestrial surfaces Moffat et al. (2007) compared 15 gap-filling techniques as applied to six European forest data sets to produce NEE. They report that MDV performed consistently moderately well. In a recent study using EC-derived fluxes over water, Shao et al. (2015) found that MDS was superior to MDV. In our case, we have an ice-covered surface for at least half of the year and have restricted directions to remove the effect of wind flowing over the island. With large gaps, especially in winter, it would be difficult to populate the bins required for LuT or MDS without a very large window; it was thought that the simple MDV, and values from other years as required, would provide estimates that are reasonable. There proved to be relatively little inter-annual variability in E caused by environmental conditions (see results). We compared our gap filled estimates using MDV with those derived from a LuT (see Supplementary Material for more details). Annual E values from MDV are larger than those from the LuT by 1–12%. We also calculated the annual E from FOR and BOG using gap-filling from a LuT. Our technique ranged between an underestimate of 3% and an overestimate of 10% depending on the year and terrestrial surface type. Our gap filled estimates therefore are likely conservative when calculating the net change in E.

2.4. Landscape level water loss estimation

We extrapolated from the tower sites using area-weighted data from the different ecosystems within the reservoir area prior to impoundment. More details can be found in Teodoru et al. (2012). The pre-flooded area classes were simplified into forest (30% cover), wetland (18%), aquatic (25%), burned forest (19%) and other non-forest (8%). FOR, BOG and BUR were used as "pre-flooded" analogues. FOR represented mature forests of all species and BOG represented wetland systems. Burns generally fall into two categories: (i) those existing on upland locations in hilly terrain or on sandy or rocky substrate where a complete burn leaves only sparse vegetation and soil; and, (ii) those on very wet, peaty substrates which results in only the primary canopy burning. In the absence of detailed information about the proportions or these two types, the total burned fraction was divided in half with BUR representing post-burn conditions in ecosystems having burned completely and now regenerating, and BOG representing post-burn conditions in ecosystems where only the canopy burned leaving understory growing in wetter, peaty soil. The remaining landscape class was attributed 50% of the E values of BUR; this non-zero value accounts for any E from sparse vegetation if present. RES represented the pre-flooded aquatic fractions (lakes, rivers and streams). For BUR, we used a year beginning in June 2011

and ending July 2012 for all study years; missing winter data at this site was taken from an average of BOG and FOR for the corresponding months.

While the pre-flooded landscape E estimation was based on a static fraction of the various terrestrial and aquatic components over the 5-years, the post-flood E extrapolation required a dynamic evaluation of the reservoir surface area during ice-free months. For the months when the reservoir was frozen (December–May), RES data was used in all years. However, reservoir management and environmental conditions result in changes to the reservoir level and therefore the evaporating surface area changes during ice-free months. The fraction of the reservoir surface represented by water is reduced when the reservoir water level is lower, resulting in exposed shorelines. Electricity demand peaks in winter in this region. Therefore, the reservoir level is lowered through the winter, recharges in spring and is typically at its highest in summer. In 2010, winter drawdown from electricity production and lower recharge resulted in low water levels remaining through much of the summer (Fig. 2). This resulted in shoreline likely being present in the tower flux footprint and therefore the measured Q_E from RES was lower than in other years because of the inclusion of non-evaporating shoreline in a source area meant exclusively to represent water. To attempt to discern or model the water fraction within the footprint would have introduced unnecessary error since the monthly E rates proved to be quite consistent between other years. As it is important to include this year that has a reduced evaporating area in subsequent analyses, we replaced the daily E for the ice-free months in 2010 with corresponding averages of the other four years.

We calculated the daily mean surface area of the reservoir based on a relationship between measured water height and reservoir water surface area developed by Hydro Quebec based on the topographic shape of the reservoir basin; daily mean reservoir height was obtained by averaging 5-min readings from a water level gauge (Accubar Constant Flow Dual Orifice Bubble Gauge, Sutron, Sterling, VA) with reported accuracy of 1 mm and located about 7 km from the reservoir power plant. We developed two scenarios for modelling the gross reservoir E. A 'static' scenario assumed that the reservoir remained at its maximum possible water height throughout all of the ice-free months (June–November) in all years and RES data was applied. This scenario provides a baseline without any management effects. A 'dynamic' scenario allowed the ice-free water level to fluctuate using the measured daily values. Wave action during the ice-free season and ice movement in the spring tends to remove and prevent vegetation growth on exposed shoreline. We assigned the fraction between maximum and the actual relative water height (exposed shoreline) a value of $E = 0$ mm and the fraction covered by water, RES. This corresponds with the findings of Tanny et al. (2011).
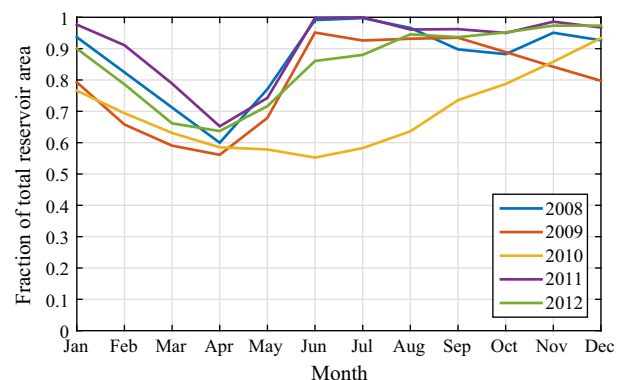

Fig. 2. Monthly reservoir area expressed as a fraction of the maximum. Ice-cover period is December through May each year.

3. Results

3.1. Climate data

Monthly average temperature in the Eastmain-1 region follows the typical pattern observed for boreal ecosystems reaching maximum and minimum mean monthly temperature in July and January, respectively. The mean November to April monthly air temperatures remain below zero (Fig. 3). The largest interannual variability in mean monthly air temperature during our study period was observed for December to February. Precipitation in the Eastmain-1 area tends to increase from the early growing season through early fall, peaking in September, and the interannual variability in precipitation is slightly greater between June to September. While the annual patterns in monthly average wind speed (standardised to a height of 10 m (U_{10}) using a power law relationship under neutral stability) were similar between the sites (Fig. 4), the wind speed measured over the reservoir was systematically higher than for the forest and the peatland. The two terrestrial sites showed similar wind speed but the peatland U_{10} was slightly higher than the forest for most months owing to the smoother surface.

3.2. Ecosystem E rates and Bowen ratios

The monthly cumulative and annual patterns of E varied among RES, FOR and BOG (Fig. 5). While all sites showed limited E during the cold season followed by an increase E coinciding with the spring melt and the start of the growing season, there was a noticeable difference in the timing of the spring increase and subsequent autumn decrease. In the spring, BOG showed the earliest E increase, followed by FOR and later by RES (Fig. 5). The opposite was observed in the fall, where BOG decreased first, followed by FOR and then RES. Overall, RES lagged the two terrestrial ecosystems. With only two partial years, BUR is not presented.

For simplicity, we will refer to the net flux of water vapour to the atmosphere in the winter as E with the understanding that a portion will be sublimation. All sites had limited E rates during the cold season, with FOR slightly higher than RES and BOG. Both the RES and BOG cold season E rates were similar with small E flux and very little day-to-day or interannual variability. Higher periods of E were measured at FOR during the winters of 2008 and 2011 (Fig. 5). The spring and early summer rates varied between years at the peatland and forest with a later increase in E rates visible in 2009.

The differences are larger in September and October where the mean E in these months for RES is 2.8 mm d^{-1}, compared with 0.7 and 1.0 for BOG and FOR, respectively. The daytime average Bowen ratio (ratio of Q_H to Q_E) was calculated and averaged monthly for the June–November period (Fig. 6). As expected, RES had the lowest Bowen ratio (period average ± standard deviation = 0.50 ± 0.46), followed by BOG (0.65 ± 0.37), and FOR (1.16 ± 0.57). RES Bowen ratio remains low but increases through the autumn as water temperature remains warm and more sensible heat is released to the
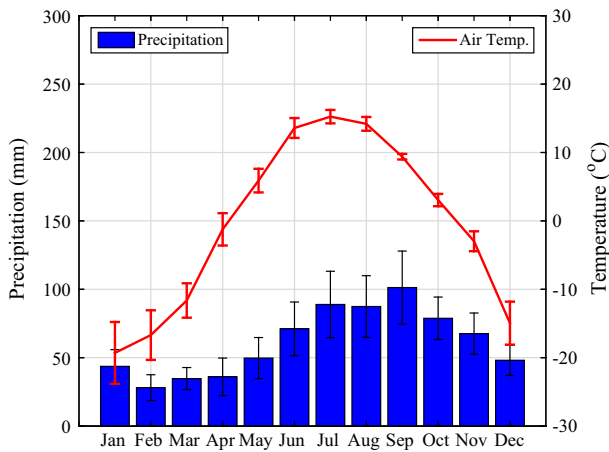

Fig. 3. The 2008–2012 monthly average temperatures (data from this study) and modelled monthly average precipitation for 1971–2000 (Hutchinson et al., 2009).
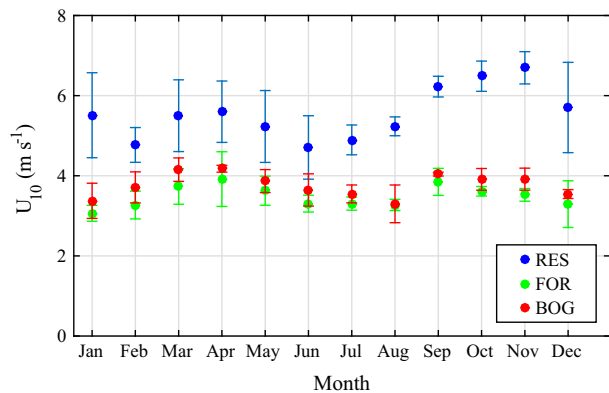

Fig. 5. Monthly evaporation at forest (FOR), peatland (BOG) and reservoir (RES) sites.

Fig. 4. Average monthly wind speed for the three tower sites over the study period. Wind speeds were standardised to 10-m height (U_{10}) assuming neutral stability. Error bars represent standard deviation.
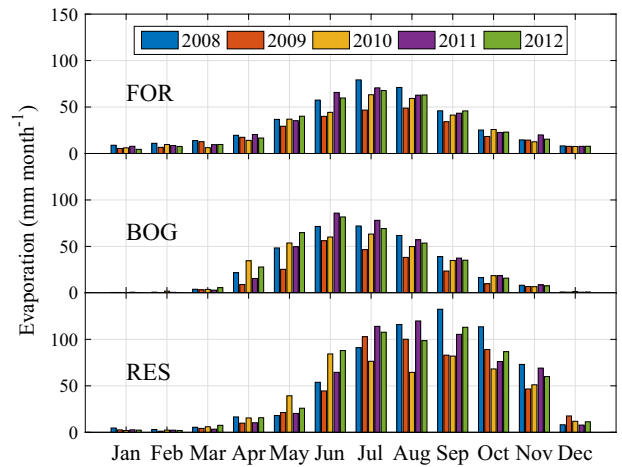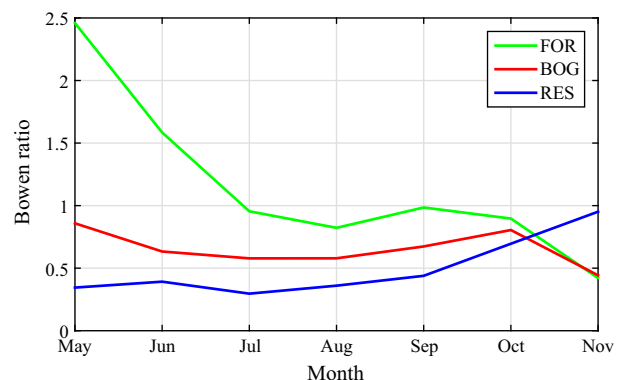

Fig. 6. Mean monthly Bowen ratio for reservoir (RES), forest (FOR) and peatland (BOG) between May and November based on daytime average values of Q_H and Q_E.

Table 3
Net cumulative evaporation (mm yr^{-1}) from the reservoir. Net is calculated as the monthly difference between weighted pre-flooded and post-flooded evapotranspiration using daily data. Pre-flooded uses weightings of 25% RES, 30% FOR, 18% BOG, 19% burned (half 'dry' = BUR; half 'wet' = BOG) and 8% non-vegetated (assigned 50% of BUR). Post-flooded was handled as follows: Ice-covered periods (December–May) were assigned RES. Open water was modelled using two scenarios: 'static' assumes that the reservoir is at its maximum water level in all years and all post-flooded surface is assigned RES; 'dynamic' uses data on the monthly average relative height of the reservoir water level. The exposed shoreline is weighted as 0 mm, and the inundated surface is assigned RES.

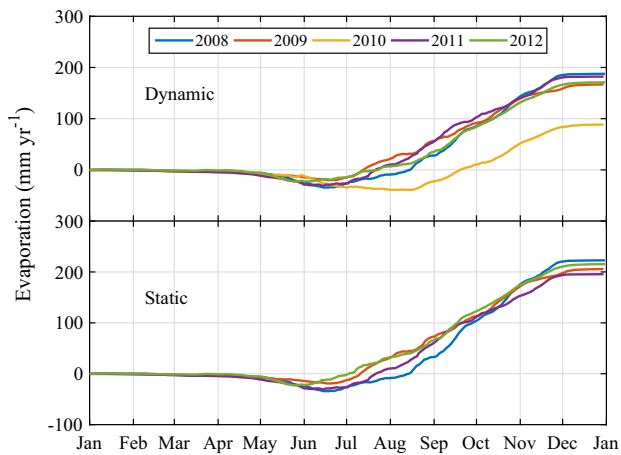| Scenario	2008	2009	2010	2011	2012	Mean	Stdev	%change
Static	218.3	201.1	n/a	195.6	206.1	205.3	9.7	52.9
Dynamic	183.0	162.3	83.9	182.1	161.8	154.6	40.8	40.4

Fig. 7. Net cumulative evaporation (mm yr^{-1}) for 2008–2012 based on daily sums. The 'dynamic' scenario allows water levels to fluctuate and any exposed shoreline evaporation is set to 0 mm. The 'static' scenario holds reservoir water height constant at its maximum value. Negative values indicate that E from the weighted pre-flooded ecosystem is greater than E from the reservoir.

cooling air. FOR Bowen ratio in contrast, starts high and falls to approximately unity as transpiration increases; values drop as autumn rainfall becomes more abundant. BOG Bowen ratio remains below unity indicating ample moisture in the peat substrate.

3.3. Net change in E

Outside of 2010 where the reservoir water level did not permit quality measurements (see Section 2.4), the cumulative annual reservoir E ranged between 523 and 636 mm yr^{-1} with the lowest and highest cumulative E observed in 2009 and 2008, respectively. E from the pre-flooded ecosystems weighted by area within the reservoir ranged between 322 and 418 mm yr^{-1}. The lowest and highest E years corresponded to 2009 and 2008 respectively.

Overall, the reservoir increased E relative to the natural ecosystem (Table 3; Fig. 7) by 40%. Most of the difference between the weighted pre-flooded ecosystem and the reservoir occurred in late summer and fall, where reservoir E rates remain high while the rates for the pre-flooded systems decrease (see Fig. 5).

4. Discussion

4.1. Site representivity

The derivation of the net change in E is predicated on the tower flux sites producing representative measurements of gross E. The 2008–2012 average daily JJA E rate at FOR was 2.0 mm d^{-1}, with a monthly average minimum and maximum of 1.5 and 2.3, respectively. These values are the same as those reported for a larch forest in eastern Siberia (1.5–2.3 mm d^{-1}; Kelliher et al., 1997; Ohta et al., 2008; Iida et al., 2009), and similar to a permafrost black

spruce forest in Alaska (0.4–2.7 mm d^{-1}; Nakai et al., 2013) and a boreal jack pine forest in central Canada (0.5–2.5 mm d^{-1}; Baldocchi et al., 1997). On an annual basis, the FOR E ranged between 282 and 392 mm, which is similar to reported values for 2-years of measurements in a black spruce forest in Saskatchewan, Canada (328–385 mm yr^{-1}; Amiro et al. (2006)). At BOG, the JJA monthly average E rates ranged from 2.3 to 3.0 mm d^{-1}, with an average of 2.6 mm d^{-1}. These numbers are similar to those reported for a blanket bog in Newfoundland, Canada (2.5 mm d^{-1}; Price, 1991), two Fens in the Hudson's Bay lowland (2.5 mm d^{-1}; Lafleur and Roulet, 1992), and the Mer Bleue bog (2.5–3.8 mm d^{-1}; Lafleur et al., 2005). The annual BOG E ranged between 221 and 363 mm, which is similar reported values from the literature (272–520 mm yr^{-1}; Lafleur et al., 2005; Sottocornola and Kiely, 2010; Wu et al., 2010; Runkle et al., 2014). The 2011 JJA average E rate at BUR was 2.1 mm d^{-1}. Amiro et al. (2006) reports values of 1–3 mm d^{-1} for a 3–4 year old burn and 3–4 mm d^{-1} for a 13–14 year old burned forest. Our seven year old burn lies appropriately within this range.

The RES average annual E (2008, 2009, 2011 and 2012) was 593 mm yr^{-1}, with a daily average for JJA of 2.9 mm d^{-1} and for Aug-Oct of 3.1 mm d^{-1}. The annual rate is similar to open water rates measured in southern Sweden (500–650 mm yr^{-1}; Van der Velde et al., 2013) and in Finland (500–700 mm yr^{-1}; Solantie and Joukola, 2001) and comparable to the measured rate of 586 mm yr^{-1} for the Robert-Bourassa reservoir in Québec (Mekonnen and Hoekstra, 2012).

4.2. Controls on E

The reservoir water temperature generally exceeds air temperature from July to December and regional wind speeds are strongest in the fall (September–November) (Fig. 8). The average wind speed over the reservoir surface is high (5.5 ms^{-1}; Fig. 4) and permits vapour and heat to be readily transported away from the surface. Mean daily Q_E exceeds Q_H for the early and middle of the ice-free season while Q_H increases through autumn until the reservoir surface freezes (Fig. 9). The lag between the time of peak radiative receipt and peak E is common in water bodies (e.g. Finch, 2001). Blanken et al. (2011) showed an extreme case where annual fluxes from Lake Superior (a cold, deep lake) were shown to be maximum in the winter and almost zero in the summer. In our case, once the reservoir is ice free, relatively high rates of E are maintained into the late autumn and early winter (Figs. 5 and 9) - far later than for the terrestrial ecosystems - and continue until the reservoir surface is fully covered by ice (by the end of December).

It is well known that E from a water surface flows along a gradient of humidity and is enhanced by wind (e.g. Brutsaert and Yu, 1968; Condie and Webster, 1997). Therefore, for the ice-free period, we would expect to find relationships between Q_E and the difference between water surface saturation vapour pressure and the air's vapour pressure [$\Delta e = (e_s(T_{wat}) - e_a)$] as well as wind speed (U). Likewise, heat flows along a temperature gradient and Q_H should be a function of the difference in water and air temperature ($\Delta T = T_{wat} - T_a$) as well as U.

We aggregated RES data biweekly over all ice-free periods in all five years. Q_H was well correlated with ΔT and U individually but very strongly correlated with their product (Fig. 10c and d); in line with theory. Q_E was best correlated with Δe but also showed strong correlation with the product $(U \cdot \Delta e)$ (Fig. 10a and b); the correlation with U alone was much weaker ($r^2 = 0.07$). These results correspond with those presented by Lenters et al. (2005); they noted that wind was out of phase with E in their multi-year study of a northern Wisconsin lake. The wind regime at our site shows a similar shift; U peaks in the early autumn and stays high while E begins to decrease. We plotted the friction velocity (u^*) against E for 30-min averages, monthly (Fig. 11). An annual hysteresis in this relationship can be seen. Minimum u^* in February over the cold frozen surface has no relationship with the small E; u^* increases as the ice melts and good relationships with E are seen during the ice-free months; relationships weaken in October and November as u^* continues to increase and E decreases.

McJannet et al. (2012) proposed a function that would account for the area of the evaporating body. Their function was not parameterized for a body as large as our reservoir, however, it did improve our regression fit marginally ($r^2 = 0.75$; data not shown). More generally, the fact that relationships between E and these environmental variables hold across years and broadly through the ice-free period indicates that (biweekly) E could be estimated with minimal measurements at this reservoir. Water temperature is routinely measured in such installations and T_a, e_a and U could be easily obtained from any standard met station on site.

When the reservoir surface freezes (December–May), there is very small E. Winter E measured at FOR was higher than for BOG or RES. Intercepted precipitation could contribute to the higher E (Molotch et al., 2007) as snow is more easily evaporated or sublimated from this more aerodynamically rough surface. Montesi et al. (2004) previously reported sublimation losses of 30% in a conifer forest. There may also be coniferous photosynthesis during brief winter warm periods resulting in transpiration of water vapour to the atmosphere (e.g. Schaberg, 2000). At BOG, the small winter E flux and the absence of interannual variability likely results from the frozen peat surface and the snow layer that generally creates a cap above the vegetation (with the exception of a few scattered small black spruce trees).

As spring approaches, E increases first at BOG. The open, exposed character of the peatland allows snow cover to melt rapidly resulting in water ponding at the surface. These shallow water accumulations are directly exposed to increasing spring sunlight and favour a more rapid increase in E rates. At FOR, the soil and understory remain covered with snow for a longer period time, as the tall, albeit sparse, black spruce trees intercept some of the
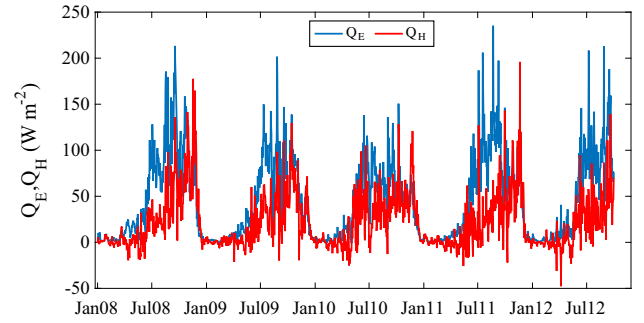

Fig. 9. Mean daily latent (Q_E) and sensible (Q_H) heat flux density from the reservoir for the five study years.
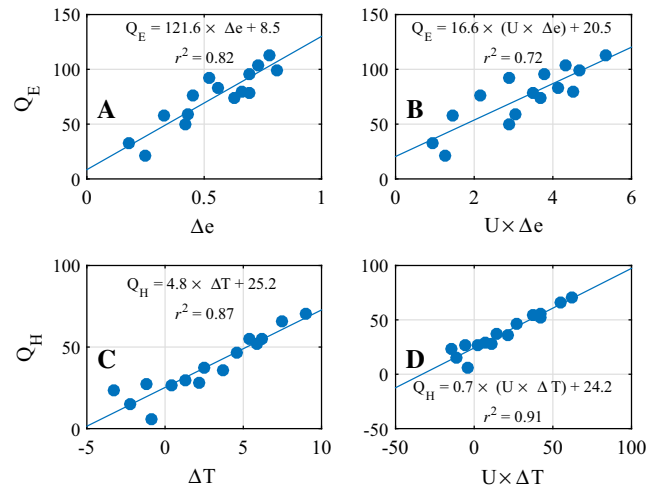

Fig. 10. Five-year, biweekly averages during the open water period of: (a) latent heat flux density (Q_E) and surface to air vapour gradient ($\Delta e = e_s(T_{wat}) - e$); (b) Q_E and the product of wind speed (U) and Δe; (c) sensible heat flux density (Q_H) and surface to air temperature gradient ($\Delta T = T_{wat} - T_a$); (d) Q_H and the product of U and ΔT.

sunlight. As the spring and early summer progress, the deciduous species leaf out in the understorey, and moisture is available in the soil. The understorey likely becomes a strong contributor to the measured E.

Both FOR and BOG experience interannual variations that seem to be linked with the prevailing weather conditions. The spring time E rate increase in 2009 is slower at both FOR and BOG
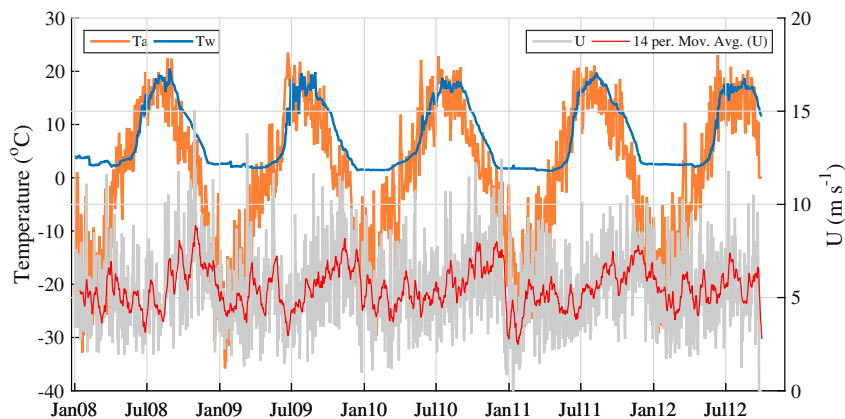

Fig. 8. Mean daily air (Ta) and water temperature (Tw), and wind speed (U) from the reservoir for the five study years.
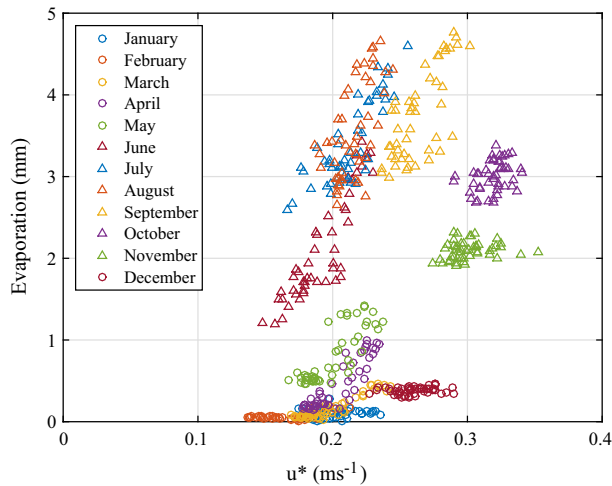
Fig. 11. Mean monthly 30-min reservoir evaporation and friction velocity ($u*$) using 2008, 09, 11, 12 combined. Circles: (partially) ice-covered months; triangles: open water months.
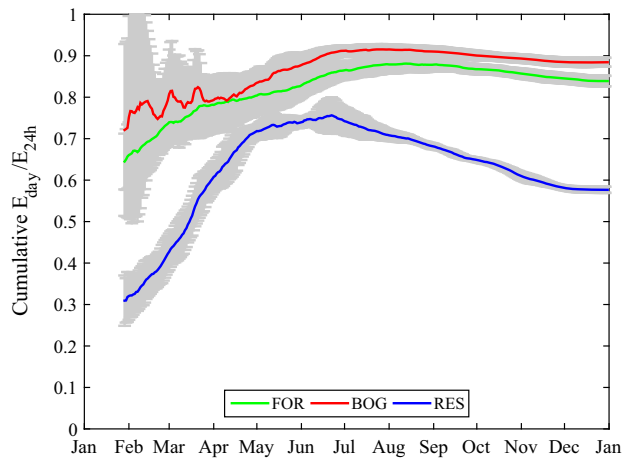

Fig. 12. Cumulative fraction of daytime period (E_{day}) to 24-h (E_{24h}) evaporation for the forest (FOR), peatland (BOG) and reservoir (RES) towers averaged over the five study years. Error bars are standard deviation of the averages.

(Fig. 5) and corresponds with lower than normal temperatures in May. Overall, a symmetrical distribution about the thermal maximum at both sites is evident but steeper at the peatland (Fig. 5). The reservoir ice cover generally lasts until the end of May and therefore prevents E from increasing as early as for the other sites. Again, the large thermal mass lags the air temperature and therefore slows down the increase in E rates (see Figs. 8 and 9). The distribution is asymmetrical as most of the E occurs in late summer and fall.

We found the relative importance of daytime (solar radiation >10 W m^{-2}) E varied between the terrestrial sites and RES. During the growing seasons, E from FOR and BOG is mediated by plant response to environmental variables and a higher proportion occurs during daytime hours. However, RES shows less of an influence of time of day as E is more driven by water to air vapour pressure differences and wind as the ice-free season progresses. Daytime values (E_{day}) were strongly correlated with 24-h values (E_{24h}) for FOR and BOG ($E_{day} = 0.91E_{24h} - 0.07$ mm d^{-1} $r^2 = 0.97$; $E_{day} = 0.94 \cdot E_{24h} - 0.05$ mm d^{-1} $r^2 = 0.99$, respectively). RES was correlated but the relationship was farther from 1:1 ($E_{day} = 0.59 \cdot E_{24h} + 0.01$ mm d^{-1} $r^2 = 0.89$). 84% of the cumulative annual E at FOR, and 88% at BOG occurs during the daytime periods while at RES, this number is 58% (Fig. 12). The decreasing

importance of E_{day} during the autumn period can clearly be seen at RES while E_{day} continues to dominate BOG and FOR. This has significant implications for the net change in E when we consider that both the rates and the timing have been changed by the creation of the reservoir.

The gross reservoir E across years is quite consistent on an annual basis and is driven largely by the ice-free period. The exception was 2009 where annual gross E is some 50 mm lower than the average of the other years. The mean water temperature for July–November, 2009 was 12.0 °C while the same period for the other years averaged 13.0 °C. However, in this colder year, the terrestrial systems were also affected and E was reduced. The result is that although the gross E from RES is lowest in 2009, the net change in E as a percentage of gross is not out of line with the other years.

4.3. Evaporative loss from hydro-electricity production in boreal regions

The long boreal winters correspond with high demand for electricity in the more southern population centres in Québec. On a calendar year, this results in a lowering of the ice-covered water level from January through May (Fig. 2). The reservoir re-fills from the point of ice breakup in May with the water covered surface slowly increasing and typically peaking in July. This changing water level in the warm season represents a challenge to the estimation of the net effect of the creation of the reservoir. Deriving a weighted pre-flooded landscape estimate and subtracting this value from the RES measurements gives the net change in E if the reservoir is at a maximum water level during all ice-free months. This 'static' scenario provides a range of cumulative net change in E between 196 and 218 mm yr^{-1}. When plotted as cumulative curves (Fig. 7), it can be seen that more water vapour is released from the pre-flooded landscape than from the reservoir until June (2012) or even mid-August (2008). This is, of course, an overestimate of the true net effect as it does not allow for management of water levels through hydro-electrical production and variability in recharge. It does, however, show that in the absence of management, the environmental effects on the net change in E are quite consistent between years with the range in annual sums being 22 mm with a coefficient of variation (CV) of 2%. In the 'dynamic' scenario, allowing for a variable water level and assigning exposed shoreline $E = 0$ mm, the cumulative net change in E ranged from 84 to 183 mm yr^{-1} and the CV increased to 12%. Here, the reservoir becomes a net emitter sometime between July and November. The lowest net emission occurs in 2010 when a combination of management and lower recharge resulted in the mean water level being much lower than the 5-yr average. In this year of lower water level, exposed shoreline that has been denuded is modelled to emit no E and therefore the result is that an active pre-reservoir vegetated surface has been partially replaced by a rocky shoreline thus reducing the net change. Nonetheless, management and natural variability will dictate that occasionally, net change in E from the reservoir will be quite small.

For a maximum reservoir area of 627 km^2 and power generation of 7.1 TW h yr^{-1}, the five-year mean gross E per unit energy production (m^3 MW h^{-1}) ranges from 39 to 53 for the 'dynamic' scenario. The gross (and net) E per unit of electricity production is of course a function of the reservoir area and the installed production level of the power house, however, these numbers are similar to those presented in a summary of gross emissions for Canadian, Austrian and Norwegian reservoirs (14–33 m^3 MW h^{-1}; Bakken et al., 2013) and for American reservoirs (34 m^3 MW h^{-1}; Wilson et al., 2012). A mean gross E of about 68 m^3 MW h^{-1} has been calculated for U.S. hydropower (Torcellini et al., 2003). Our values are much lower than mean gross values for reservoirs in temperate, tropical and warm-dry regions, which are 152 m^3 MW h^{-1},

498 m^3 MW h^{-1} and 1658 m^3 MW h^{-1}, respectively (Bakken et al., 2013). Using the net (reservoir – weighted ecosystems pre-flooding) E reduces these substantially. The net annual evaporative loss per unit energy produced was 7–16 m^3 MW h^{-1}, with an average of 14 m^3 MW h^{-1}. The five-year mean net E ranges from 19% to 34% of the gross E. Management decisions directly impact the water released to the atmosphere through reductions in the evaporative surface of the reservoir. These values are well within the range of the limited number of studies reporting net E in New Zealand (12–60%; Herath et al., 2011), Ethiopia (32–58%; Yesuf, 2012) and Austria (30%; Demeke et al., 2013).

5. Conclusion

The creation of a reservoir for hydroelectric production in the Boreal region results in an annual increase in E to the atmosphere. As population increases and economic growth continues, water demand will grow (Ercin and Hoekstra, 2014). To determine the evaporative water loss of a Boreal hydroelectric reservoir, the development of an appropriate and common methodology is required. Terrestrial ecosystems are sources of water vapour to the atmosphere and therefore, unlike carbon (Teodoru et al., 2012), the system does not shift from sink to source following the land use change. The gross E from the pre-existing composite surface needs to therefore be subtracted from the measured gross E from the reservoir. The resulting net E is then the true measure of the effect of the reservoir.

The creation of a hydroelectric reservoir alters the water vapour exchange processes between the surface and the atmosphere. Flooding the Boreal landscape means that forests, peatlands and aquatic features are replaced by a large water surface. Terrestrial surfaces which predominantly gave off E during daytime periods are replaced by a surface which continues to evaporate at night during ice-free periods. The thermal lag of the water permits E rates that exceed the terrestrial sites well into the autumn period.

However, the reservoir is not a static water body with fixed surface area. Management of water levels for electricity production and the natural variability in temperature and precipitation combine to result in a varying reservoir water level and therefore the resulting fraction of evaporating surface needs to be considered during ice-free periods. As the reservoir water levels lower, the net E is reduced as an increasing amount of non-evaporating shoreline is exposed. Overall, the interannual effect of meteorological conditions on the net change in E was less than the effect of management.

Acknowledgements

Appendix A. Supplementary material

Supplementary data associated with this article can be found, in the online version, at http://dx.doi.org/10.1016/j.jhydrol.2016.06.067.

References

Amiro, B.D., Barr, A.G., Black, T.A., Iwashita, H., Kljun, N., McCaughey, J.H., Morgenstern, K., Murayama, S., Nesic, Z., Orchansky, A.L., Saigusa, N., 2006. Carbon, energy and water fluxes at mature and disturbed forest sites, Saskatchewan, Canada. Agric. For. Meteorol. 136, 237–251. http://dx.doi.org/10.1016/j.agrformet.2004.11.012.

Anderson, R.J., Smith, S.D., 1981. Evaporation coefficient for the sea surface from eddy flux measurements. J. Geophys. Res. 86 (C1), 449–456. http://dx.doi.org/10.1029/JC086iC01p00449.

Assouline, S., Mahrer, O., 1993. Evaporation from Lake Kinneret: 1. Eddy correlation system measurements and energy budget estimates. Water Resour. Res. 29 (4), 901–910. http://dx.doi.org/10.1029/92WR02432.

Assouline, S., Tyler, S.W., Tanny, J., Cohen, S., Bou-Zeid, E., Parlange, M.B., Katul, G.G., 2008. Evaporation from three water bodies of different sizes and climates: measurements and scaling analysis. Adv. Water Res. 31 (1), 160–172.

Bakken, T.H., Killingtveit, Å., Engeland, K., Alfredsen, K., Harby, A., 2013. Water consumption from hydropower plants – review of published estimates and an assessment of the concept. Hydrol. Earth Syst. Sci. 17, 3983–4000. http://dx.doi.org/10.5194/hess-17-3983-2013.

Baldocchi, D.D., 2003. Assessing the eddy covariance technique for evaluating carbon dioxide exchange rates of ecosystems: past, present and future. Glob. Change Biol. 9, 479–492.

Baldocchi, D.D., Vogel, C.A., Hall, B., 1997. Seasonal variation of energy and water vapor exchange rates above and below a boreal jack pine forest canopy. J. Geophys. Res.-Atmos. 102, 28939–28951.

Bergeron, O., Strachan, I.B., 2011. CO$_2$ sources and sinks in urban and suburban areas of a northern mid-latitude city. Atmos. Environ. 45, 1564–1573.

Beyrich, F., Leps, J.-P., Mauder, M., Bange, J., Foken, T., Huneke, S., Lohse, H., Ludi, A., Meijninger, W.M.L., Mironov, D., Weisensee, U., Zittel, P., 2006. Area-averaged surface fluxes over the LITFASS region based on eddy-covariance measurements. Bound.-Lay. Meteorol. 121, 33–65. http://dx.doi.org/10.1007/s10546-006-9052-x.

Blanken, P.D., Rouse, W.R., Culf, A.D., Spence, C., Boudreau, D., Jasper, J.N., Kochtubajda, B., Schertzer, W.M., Marsh, P., Verseghy, D., 2000. Eddy covariance measurements of evaporation from Great Slave Lake, Northwest Territories, Canada. Water Resour. Res. 36 (4), 1069–1077. http://dx.doi.org/10.1029/1999WR900338.

Blanken, P.D., Rouse, W.R., Schertzer, W.M., 2003. Enhancement of evaporation from a large northern lake by the entrainment of warm, dry air. J. Hydrometeorol. 4, 680–693. http://dx.doi.org/10.1175/1525-7541(2003)004<0680:EOEFAL>2.0.CO;2.

Blanken, P.D., Spence, C., Hedstrom, N., Lenters, J.D., 2011. Evaporation from Lake Superior: 1. Physical controls and processes. J. Great Lakes Res. 37, 707–716.

Brutsaert, W., Yu, S.L., 1968. Mass transfer aspects of pan evaporation. J. Appl. Meteorol. 7, 563–566.

Buffam, I., Turner, M.G., Desai, A.R., Hanson, P.C., Rusak, J.A., Lottig, N.R., Stanley, E.H., Carpenter, E.H., 2011. Integrating aquatic and terrestrial components to construct a complete carbon budget of a north temperate lake district. Glob. Change Biol. http://dx.doi.org/10.1111/j.1365-2486.2010.02313.x.

Condie, S.A., Webster, I.T., 1997. The influence of wind stress, temperature, and humidity gradients on evaporation from reservoirs. Water Resour. Res. 33, 2813–2822.

DeCosmo, J., Katsaros, K.B., Smith, S.D., Anderson, R.J., Oost, W.A., Bumke, K., Chadwick, H., 1996. Air-sea exchange of water vapor and sensible heat: the Humidity Exchange Over the Sea (HEXOS) results. J. Geophys. Res. 101 (C5), 12001–12016. http://dx.doi.org/10.1029/95JC03796.

Demeke, T.A., Marence, M., Mynett, A.E., 2013. Evaporation from reservoirs and the hydropower water footprint. Proc. Afr. 2013, 16–18.

Eichlinger, W.E., Nichols, J., Prueger, J.H., Hipps, L.E., Neale, C.M.U., Cooper, D.I., Bawazir, A.S., 2003. Lake evaporation estimates in arid environments. IIHR Report No. 430, University of Iowa, Iowa City, IA.

Ercin, A.E., Hoekstra, A.Y., 2014. Water footprint scenarios for 2050: a global analysis. Environ. Int. 64, 71–82.

Falge, E., Baldocchi, D., Olson, R., Anthoni, P., Aubinet, M., Bernhofer, C., Burba, G., Ceulemans, R., Clement, R., Dolman, H., Granier, A., Gross, P., Grünwald, T., Hollinger, D., Jensen, N.-O., Katul, G., Keronen, P., Kowalski, A., Lai, C.T., Law, B.E., Meyers, T., Moncrieff, J., Moors, E., Munger, J.W., Pilegaard, K., Rannik, U., Rebmann, C., Suyker, A., Tenhunen, J., Tu, K., Verma, S., Vesala, T., Wilson, K., Wofsy, S., 2001. Gap filling strategies for defensible annual sums of net ecosystem exchange. Agric. For. Meteorol. 107, 43–69.

Finch, J.W., 2001. A comparison between measured and modelled open water evaporation from a reservoir in south-east England. Hydrol. Process. 15, 2771–2778. http://dx.doi.org/10.1002/hyp.267.

Friehe, C.A., Schmitt, K.F., 1976. Parameterization of air-sea interface fluxes of sensible heat and moisture by the bulk aerodynamic formulas. J. Phys. Oceanogr. 6, 801–809. http://dx.doi.org/10.1175/1520-0485(1976)006<0801:POASIF>2.0.CO;2.

Heikinheimo, M., Kangas, M., Tourula, T., Venäläinen, A., Tattari, S., 1999. Momentum and heat fluxes over lakes Tämnaren and Råksjö determined by the bulk-aerodynamic and eddy-correlation methods. Agric. For. Meteorol. 98–99, 521–534. http://dx.doi.org/10.1016/S0168-1923(99)00121-5.

Herath, I., Deurer, M., Horne, D., Singh, R., Clothier, B., 2011. The water footprint of hydroelectricity: a methodological comparison from a case study in New Zealand. J. Clean. Prod. 19, 1582–1589.

Humphreys, E.R., Lafleur, P.M., Flanagan, L.B., Hedstrom, N., Syed, K.H., Glenn, A.J., Granger, R., 2006. Summer carbon dioxide and water vapor fluxes across a range of northern peatlands. J. Geophys. Res. 111, G04011. http://dx.doi.org/10.1029/2005JG000111.

Hutchinson, M.F., McKenney, D.W., Lawrence, K., Pedlar, J.H., Hopkinson, R.F., Milewska, E., Papadopol, P., 2009. Development and testing of Canada-wide interpolated spatial models of daily minimum–maximum temperature and precipitation for 1961–2003. J. Appl. Meteor. Climatol. 48, 725–741. http://dx.doi.org/10.1175/2008JAMC1979.1.

Iida, S., Ohta, T., Matsumoto, K., Nakai, T., Kuwada, T., Kononov, A.V., Maximov, T.C., van der Molen, M.K., Dolman, H., Tanaka, H., Yabuki, H., 2009. Evapotranspiration from understory vegetation in an eastern Siberian boreal larch forest. Agric. For. Meteorol. 149, 1129–1139. http://dx.doi.org/10.1016/j.agrformet.2009.02.003.

Ikebuchi, S., Seki, M., Ohtoh, A., 1988. Evaporation from Lake Biwa. J. Hydrol. 102, 427–449. http://dx.doi.org/10.1016/0022-1694(88)90110-2.

Jarvis, P.G., McNaughton, K.G., 1986. Stomatal Control of Transpiration: Scaling Up from Leaf to Region. In: MacFadyen, A., Ford, E.D. (Eds.), Advances in Ecological Research. Academic Press, pp. 1–49.

Jassal, R.S., Black, T.A., Spittlehouse, D.L., Brümmer, C., Nesic, Z., 2009. Evapotranspiration and water use efficiency in different-aged Pacific Northwest Douglas-fir stands. Agric. For. Meteorol. 149, 1168–1178. http://dx.doi.org/10.1016/j.agrformet.2009.02.004.

Jonsson, A., Åberg, J., Lindroth, A., Jansson, M., 2008. Gas transfer rate and CO_2 flux between an unproductive lake and the atmosphere in northern Sweden. J. Geophys. Res. 113, G04006. http://dx.doi.org/10.1029/2008JG000688.

Katsaros, K.B., Smith, S.D., Oost, W.A., 1987. HEXOS - Humidity EXchange Over the Sea; a program for research on water-vapor and droplet fluxes from sea of air at moderate to high wind speeds. Bull. Amer. Meteorol. Soc. 68 (5), 466–476. http://dx.doi.org/10.1175/1520-0477(1987)068<0466:HEOTSA>2.0.CO;2.

Kelliher, F.M., Hollinger, D.Y., Schulze, E.-D., Vygodskaya, N.N., Byers, J.N., Hunt, J.E., McSeveny, T.M., Milukova, I., Sogatchev, A., Varlargin, A., Ziegler, W., Arneth, A., Bauer, G., 1997. Evaporation from an eastern Siberian larch forest. Agric. For. Meteorol. 85, 135–147. http://dx.doi.org/10.1016/S0168-1923(96)02424-0.

Kurbatova, J., Arneth, A., Vygodskaya, N.N., Kolle, O., Varlargin, A.V., Milyukova, I.M., Tchebakova, N.M., Schulze, E.-D., Lloyd, J., 2002. Comparative ecosystem-atmosphere exchange of energy and mass in a European Russian and a central Siberian bog I. Interseasonal and interannual variability of energy and latent heat fluxes during the snowfree period. Tellus B 54, 497–513. http://dx.doi.org/10.1034/j.1600-0889.2002.01354.x.

Lafleur, P.M., Hember, R.A., Admiral, S.W., Roulet, N.T., 2005. Annual and seasonal variability in evapotranspiration and water table at a shrub-covered bog in southern Ontario, Canada. Hydrol. Process. 19, 3533–3550. http://dx.doi.org/10.1002/hyp.5842.

Lafleur, P.M., Roulet, N.T., 1992. A comparison of evaporation rates from two fens of the Hudson Bay Lowland. Aquat. Bot. 44, 59–69. http://dx.doi.org/10.1016/0304-3770(92)90081-S.

Lenters, J.D., Kratz, T.K., Bowser, C.J., 2005. Effects of climate variability on lake evaporation: Results from a long-term energy budget study of Sparkling Lake, northern Wisconsin (USA). J. Hydrol. 308, 168–195.

Liu, H., Zhang, Y., Liu, S., Jiang, H., Sheng, L., Williams, Q.L., 2009. Eddy covariance measurements of surface energy budget and evaporation in a cool season over southern open water in Mississippi. J. Geophys. Res. 114, D04110. http://dx.doi.org/10.1029/2008JD010891.

Liu, H., Blanken, P.D., Weidinger, T., Nordbo, A., Vesala, T., 2011. Variability in cold front activities modulating cool-season evaporation from a southern inland water in the USA. Environ. Res. Lett. 6 (024022), 8. http://dx.doi.org/10.1088/1748-9326/6/2/024022.

Liu, H., Zhang, Q., Dowler, G., 2012. Environmental controls on the surface energy budget over a large southern inland water in the United States: an analysis of one-year eddy covariance flux data. J. Hydrometeorol. 13, 1893–1910. http://dx.doi.org/10.1175/JHM-D-12-020.1.

McGloin, R., McGowan, H., McJannet, D., Cook, F., Sogachev, A., Burn, S., 2014. Quantification of surface energy fluxes from a small water body using scintillometry and eddy covariance. Water Resour. Res. 50, 494–513. http://dx.doi.org/10.1002/2013WR013899.

McGowan, H.A., Sturman, A.P., MacKellar, M.C., Wiebe, A.H., Neil, D.T., 2010. Measurements of the local energy balance over a coral reef flat, Heron Island, southern Great Barrier Reef, Australia. J. Geophys. Res. 115, D19124. http://dx.doi.org/10.1029/2010JD014218.

McJannet, D.L., Cook, F.J., McGloin, R.P., McGowan, H.A., Burn, S., 2011. Estimation of evaporation and sensible heat flux from open water using a large-aperture scintillometer. Water Resour. Res. 47, W05545. http://dx.doi.org/10.1029/2010WR010155.

McJannet, D.L., Webster, I.T., Cook, F.J., 2012. An area-dependent wind function for estimating open water evaporation using land-based meteorological data. Environ. Modell. Softw. 31, 76–83.

McLaren, J.D., Arain, M.A., Khomik, M., Peichl, M., Brodeur, J., 2008. Water flux components and soil water-atmospheric controls in a temperate pine forest growing in a well-drained sandy soil. J. Geophys. Res. 113, G04031. http://dx.doi.org/10.1029/2007JG000653.

McMahon, T.A., Peel, M.C., Lowe, L., Srikanthan, R., McVicar, T.R., 2013. Estimating actual, potential, reference crop and pan evaporation using standard meteorological data: a pragmatic synthesis. Hydrol. Earth Syst. Sci. 17, 1331–1363. http://dx.doi.org/10.5194/hess-17-1331-2013.

McVicar, T.R., Roderick, M.L., Donohue, R.J., Li, L.T., Van Niel, T.G., Thomas, A., Grieser, J., Jhajharia, D., Himri, Y., Mahowald, N.M., Mescherskaya, A.V., Kruger, A.C., Rehman, S., Dinpashoh, Y., 2012. Global review and synthesis of trends in observed terrestrial near-surface wind speeds: implications for evaporation. J. Hydrol. 416–417, 182–205. http://dx.doi.org/10.1016/j.jhydrol.2011.10.024.

Mekonnen, M.M., Hoekstra, A.Y., 2012. The blue water footprint of electricity from hydropower. Hydrol. Earth Syst. Sci. 16, 179–187. http://dx.doi.org/10.5194/hess-16-179-2012.

Mengistu, M.G., Savage, M.J., 2010. Open water evaporation estimation for a small shallow reservoir in winter using surface renewal. J. Hydrol. 380 (1–2), 27–35. http://dx.doi.org/10.1016/j.jhydrol.2009.10.014.

Mkhabela, M.S., Amiro, B.D., Barr, A.G., Black, T.A., Hawthorne, I., Kidston, J., McCaughey, J.H., Orchansky, A.L., Nesic, Z., Sass, A., Shashkov, A., Zha, T., 2009. Comparison of carbon dynamics and water use efficiency following fire and harvesting in Canadian boreal forests. Agric. For. Meteorol. 149 (783–794), 2008. http://dx.doi.org/10.1016/J.Agrformet.10.025.

Moffat, A.M., Papale, D., Reichstein, M., Hollinger, D.Y., Richardson, A.D., Barr, A.G., Beckstein, C., Braswell, B.H., Churkina, G., Desai, A.R., Falge, E., Gove, J.H., Heimann, M., Hui, D., Jarvis, A.J., Kattge, J., Noormets, A., Stauch, V.J., 2007. Comprehensive comparison of gap-filling techniques for eddy covariance net carbon fluxes. Agric. For. Meteorol. 147, 209–232.

Molotch, N.T., Blanken, P.D., Williams, M.W., Turnipseed, A.A., Monson, R.K., Margulis, S.A., 2007. Estimating sublimation of intercepted and sub-canopy snow using eddy covariance systems. Hydrol. Process. 21, 1567–1575.

Montesi, J., Elder, K., Schmidt, R.A., Davis, R.E., 2004. Sublimation of intercepted snow within a subalpine forest canopy at two elevations. J. Hydrometeorol. 5, 763–773.

Nakai, T., Kim, Y., Busey, R.C., Suzuki, R., Nagai, S., Kobayashi, H., Park, H., Sugiura, K., Ito, A., 2013. Characteristics of evapotranspiration from a permafrost black spruce forest in interior Alaska. Polar Sci. 7, 136–148. http://dx.doi.org/10.1016/j.polar.2013.03.003.

Nordbo, A., Launiainen, S., Mammarella, I., Leppäranta, M., Huotari, J., Ojala, A., Vesala, T., 2011. Long-term energy flux measurements and energy balance over a small boreal lake using eddy covariance technique. J. Geophys. Res. 116, D02119. http://dx.doi.org/10.1029/2010JD014542.

Ohta, T., Maximov, T.C., Dolman, A.J., Nakai, T., van der Molen, M.K., Kononov, A.V., Maximov, A.P., Hiyama, T., Iijima, Y., Moors, E.J., Tanaka, H., Toba, T., Yabuki, H., 2008. Interannual variation of water balance and summer evapotranspiration in an eastern Siberian larch forest over a 7-year period (1998–2006). Agric. For. Meteorol. 148, 1941–1953. http://dx.doi.org/10.1016/j.agrformet.2008.04.012.

Panin, G.N., Nasonov, A.E., Foken, T., Lehse, H., 2006. On the parameterisation of evaporation and sensible heat exchange for shallow lakes. Theor. Appl. Climatol. 85 (5), 123–129.

Papale, D., Reichstein, M., Aubinet, M., Canfora, E., Bernhofer, C., Kutsch, W., Longdoz, B., Rambal, S., Valentini, R., Vesala, T., Yakir, D., 2006. Towards a standardized processing of net ecosystem exchange measured with eddy covariance technique: algorithms and uncertainty estimation. Biogeosciences 3, 571–583.

Pelletier, L., Garneau, M., Moore, T.R., 2011. Variation in CO_2 exchange over three summers at microform scale in a boreal bog, Eastmain region, Québec, Canada. J. Geophys. Res. 116, G03019. http://dx.doi.org/10.1029/2011JG001657.

Penman, H.L., 1948. Natural evaporation from open water, bare soil and grass. Proc. Roy. Soc. London A 193, 120–145. http://dx.doi.org/10.1098/rspa.1948.0037.

Price, J.S., 1991. Evaporation from a blanket bog in a foggy coastal environment. Bound.-Lay. Meteorol. 57, 391–406. http://dx.doi.org/10.1007/BF00120056.

Rouse, W.R., Blanken, P.D., Bussières, N., Walker, A.E., Oswald, C.J., Schertzer, W.M., Spence, C., 2008. An investigation of the thermal and energy balance regimes of Great Slave and Great Bear Lakes. J. Hydrometeorol. 9 (6), 1318–1333.

Rouse, W.R., Oswald, C.M., Binyamin, J., Blanken, P.D., Schertzer, W.M., Spence, C., 2003. Interannual and seasonal variability of the surface energy balance and temperature of central Great Slave Lake. J. Hydrometeorol. 4, 720–730. http://dx.doi.org/10.1175/1525-7541(2003)004<0720:IASVOT>2.0.CO;2.

Runkle, B.R.K., Wille, C., Gažovič, M., Wilmking, M., Kutzbach, L., 2014. The surface energy balance and its drivers in a boreal peatland fen of northwestern Russia. J. Hydrol. 511, 359–373. http://dx.doi.org/10.1016/j.jhydrol.2014.01.056.

Schaberg, P.G., 2000. Winter photosynthesis in red spruce (Picea rubens Sarg.): Limitations, potential benefits, and risks. Arc. Antarc. Alp. Res. 32, 375–380. http://dx.doi.org/10.2307/1552385.

Sene, K.J., Gash, J.H.C., McNeil, D.D., 1991. Evaporation from a tropical lake: comparison of theory with direct measurements. J. Hydrol. 127 (1–4), 193–217. http://dx.doi.org/10.1016/0022-694(91)90115-X.

Shao, C., Chen, J., Stepien, C.A., Chu, H., Ouyang, Z., Bridgeman, T.B., Czajkowski, K.P., Becker, R.H., John, R., 2015. Diurnal to annual changes in latent, sensible heat, and CO_2 fluxes over a Laurentian Great Lake: a case study in Western Lake Erie. J. Geophys. Res. Biogeosci. 120, 1587–1604. http://dx.doi.org/10.1002/2015JG003025.

Smith, S.D., 1974. Eddy flux measurements over Lake Ontario. Bound.-Lay. Meteorol. 6, 235–255.

Smith, S.D., 1989. Water vapour flux at the sea surface. Bound.-Lay. Meteorol. 47, 277–293.

Solantie, R.K., Joukola, M.P., 2001. Evapotranspiration 1961–1990 in Finland as function of meteorological and land-type factors. Boreal Environ. Res. 6, 261–273.

Sottocornola, M., Kiely, G., 2010. Energy fluxes and evaporation mechanisms in an Atlantic blanket bog in southwestern Ireland. Water Resour. Res. 46, W11524. http://dx.doi.org/10.1029/2010WR009078.

Spence, C., Blanken, P.D., Lenters, J.D., Hedstrom, N., 2013. The importance of spring and autumn atmospheric conditions for the evaporation regime of Lake Superior. J. Hydrometeorol. 14, 1647–1658. http://dx.doi.org/10.1175/JHM-D-12-0170.1.

Spence, C., Hedstrom, N., 2015. Attributes of Lake Okanagan evaporation and development of a mass transfer model for water management purposes. Can. Water Resour. J. 40 (3), 250–261. http://dx.doi.org/10.1080/07011784.2015.1046140.

Strachan, I.B., Pelletier, L., Bonneville, M.-C., 2016. Interannual variability in water table depth controls net ecosystem carbon dioxide exchange in a boreal peatland. Biogeochemistry 127, 99–111.

Stannard, D.I., Rosenberry, D.O., 1991. A comparison of short-term measurements of lake evaporation using eddy correlation and energy budget methods. J. Hydrol. 122 (1–4), 15–22. http://dx.doi.org/10.1016/0022-1694(91)90168-H.

Tanaka, H., Hiyama, T., Nakamura, K., 2008. Turbulent flux observations at the tip of a narrow cape on Miyako Island in Japan's southwestern islands. J. Meteorol. Soc. Japan, Ser. II 86 (5), 649–667. http://dx.doi.org/10.2151/jmsj.86.649.

Tanny, J., Cohen, S., Assouline, S., Lange, F., Grava, A., Berger, D., Teltch, B., Parlange, M.B., 2008. Evaporation from a small water reservoir: direct measurements and estimates. J. Hydrol. 351 (1–2), 218–229. http://dx.doi.org/10.1016/j.jhydrol.2007.12.012.

Tanny, J., Cohen, S., Berger, D., Teltch, B., Mekhmandarov, Y., Bahar, M., Katul, G.G., Assouline, S., 2011. Evaporation from a reservoir with fluctuating water level: correcting for limited fetch. J. Hydrol. 404, 146–156. http://dx.doi.org/10.1016/j.jhydrol.2011.04.025.

Teodoru, C.R., Bastien, J., Bonneville, M.C., del Giorgio, P.A., Demarty, M., Garneau, M., Helie, J.F., Pelletier, L., Prairie, Y.T., Roulet, N.T., Strachan, I.B., Tremblay, A., 2012. The net carbon footprint of a newly created boreal hydroelectric reservoir. Global Biogeochem. Cy. 26, GB2016. http://dx.doi.org/10.1029/2011GB004187.

Torcellini, P., Long, N., Judkoff, R., 2003. Consumption water use for U.S. power production. NREL/TP-550-33905, National Renewable Energy Laboratory, USA.

Van Bellen, S., Dallaire, P.-L., Garneau, M., Bergeron, Y., 2011. Quantifying spatial and temporal Holocene carbon accumulation in ombrotrophic peatlands of the Eastmain region, Quebec, Canada. Global Biogeochem. Cy. 25, GB2016. http://dx.doi.org/10.1029/2010GB003877.

Van der Velde, Y., Lyon, S.W., Destouni, G., 2013. Data-driven regionalization of river discharges and emergent land cover–evapotranspiration relationships across Sweden. J. Geophys. Res. Atmos. 118, 2576–2587. http://dx.doi.org/10.1002/jgrd.50224.

Venäläinen, A., Heikinheimo, M., Tourula, T., 1998. Latent heat flux from small sheltered lakes. Bound.-Lay. Meteorol. 86 (3), 355–377.

Vesala, T., Huotari, J., Rannik, Ü., Suni, T., Smolander, S., Sogachev, A., Launiainen, S., Ojala, A., 2006. Eddy covariance measurements of carbon exchange and latent and sensible heat fluxes over a boreal lake for a full open-water period. J. Geophys. Res. 111, D11101. http://dx.doi.org/10.1029/2005JD006365.

Vesala, T., Eugster, W., Ojala, A., 2012. Eddy covariance measurements over lakes. In: Aubinet, M., Vesala, T., Papale, D. (Eds.), Eddy Covariance, a Practical Guide to Measurement and Data Analysis. Springer.

Vickers, D., Mahrt, L., 1997. Quality control and flux sampling problems for tower and aircraft data. J. Atmos. Ocean. Tech. 14, 512–526. http://dx.doi.org/10.1175/1520-0426(1997)014<0512:QCAFSP>2.0.CO;2.

Webb, E.K., Pearman, G.I., Leuning, R., 1980. Correction of flux measurements for density effects due to heat and water-vapor transfer. Quart. J. Roy. Meteorol. Soc. 106, 85–100.

Wilson, W., Leipzug, T., Griffiths-Sattenspiel, B., 2012. Burning our rivers: the water footprint of electricity. A River Network Report, Rivers, Energy & Climate Change Program. River Network <http://www.rivernetwork.org/>.

Wu, J., Kutzbach, L., Jager, D., Wille, C., Wilmking, M., 2010. Evapotranspiration dynamics in a boreal peatland and its impact on the water and energy balance. J. Geophys. Res. 115, G04038. http://dx.doi.org/10.1029/2009JG001075.

Xiao, W., Liu, S., Wang, W., Yang, D., Xu, J., Cao, C., Li, H., Lee, X., 2013. Transfer coefficients of momentum, heat and water vapour in the atmospheric surface layer of a large freshwater lake. Bound.-Lay. Meteorol. 148 (3), 479–494.

Yesuf, M.B., 2012. Impacts of cascade hydropower plants on the flow of the river system and water level in Lake Turkana in Omo-Ghibe catchment, Ethiopia. M. Sc. thesis Norwegian University of Science and Technology, Trondheim, Norway.